Mixed Cobaltocenium−Ferrocene Heterobimetallic Complexes and Their Binding Interactions with β-Cyclodextrin. A Three-State, Host−Guest System under Redox Control

Blanca González,[†] Isabel Cuadrado,*[,†] Beatriz Alonso,[†] Carmen M. Casado,[†] Moisés Morán,[†] and Angel E. Kaifer*[,§]

Departamento de Química Inorgánica, Facultad de Ciencias, Universidad Autónoma de Madrid, Cantoblanco, 28049-Madrid, Spain, and Center for Supramolecular Science, Department of Chemistry, University of Miami, Coral Gables, Florida 33124-0431

Received March 14, 2002

A new organometallic compound (**2**) containing a cobaltocenium and a ferrocene residue was synthesized, and its structure was determined by X-ray diffraction methods. The two metallocene subunits in **2** are linked by a connector featuring a positively charged quaternary ammonium nitrogen atom, which increases the aqueous solubility of **2** in every oxidation state, as compared to the previously reported heterobimetallic cobaltocenium−ferrocene complex **1**, which has an uncharged tether. The electrochemical behavior of **1** and **2** in 0.1 M NaCl is characterized by the reversible one-electron oxidation of the ferrocene residue and by the one-electron reduction of the cobaltocenium subunit. The latter electrochemical process is reversible only in **2**. In compound **1**, the voltammetric reduction wave is distorted by precipitation of the fully reduced form on the electrode surface. Both compounds exhibit three accessible oxidation states that can be represented as Fc^+-Cob^+, Fc-Cob^+, and Fc-Cob. Cyclic voltammetric experiments in the presence of the host β-cyclodextrin (β-CD) reveal that the fully oxidized form, Fc^+-Cob^+, is not bound, the intermediate oxidation state Fc-Cob^+ forms a stable complex by inclusion of its ferrocene site, and the fully reduced form, Fc-Cob, presents two binding sites for the CD host. The voltammetric behavior was analyzed using digital simulation techniques in order to obtain the thermodynamic parameters for the binding equilibria.

Introduction

The binding interactions between ferrocene derivatives and β-cyclodextrin (β-CD) have been extensively investigated.[1−10] Recently, this host−guest pair was also selected for an investigation using dynamic single molecule force spectroscopy.[11] In general terms, ferrocene residues are bound by β-CD, while the oxidized, positively charged ferrocenium forms do not form stable complexes.[12] We have recently investigated this host−guest pair in a number of dendrimer systems.[13,14] In similar fashion, cobaltocenium derivatives are not bound by β-CD, but give rise to stable inclusion complexes upon one-electron reduction to their neutral cobaltocene forms.[15] We have also utilized this host−guest system in a dendrimer system.[16] Our interest in dendrimers functionalized with multiple metallocene centers on their peripheries has led us to prepare mixed systems containing both ferrocene and cobaltocenium residues.[17,18] In this report, we focus our attention on two mixed metallocene heterobimetallic complexes, com-

* Corresponding author. Tel: (305) 284-3468. Fax: (305) 444-1777 or (305) 284-4571. Internet: akaifer@miami.edu.
[†] Universidad Autónoma de Madrid.
[§] University of Miami.

(1) Harada, A.; Takahashi, S. *J. Chem. Soc., Chem. Commun.* **1984**, 645.
(2) Menger, F. M.; Sherrod, M. J. *J. Am. Chem. Soc.* **1988**, *110*, 8606.
(3) Thiem, H.-J.; Brandl, M.; Breslow, R. *J. Am. Chem. Soc.* **1988**, *110*, 8612.
(4) Breslow, R.; Czarniecki, M. F.; Emert, J.; Hamaguchi, H. *J. Am. Chem. Soc.* **1980**, *102*, 762.
(5) Sigel, B.; Breslow, R. *J. Am. Chem. Soc.* **1975**, *97*, 6869.
(6) Matsue, T.; Evans, D. H.; Osa, T.; Kobayashi, N. *J. Am. Chem. Soc.* **1985**, *107*, 3411.
(7) Isnin, R.; Salam, C.; Kaifer, A. E. *J. Org. Chem.* **1991**, *56*, 35.
(8) Godínez, L. A.; Patel, S.; Criss, C. M.; Kaifer, A. E. *J. Phys. Chem.* **1995**, *99*, 17449.
(9) Coutouli-Argyropoulou, E.; Kelaidopoulou, A.; Sideris, C.; Kokkinidis, G. *J. Electroanal. Chem.* **1999**, *477*, 130.
(10) Osella, D.; Carretta, A.; Nervi, C.; Ravera, M.; Gobetto, R. *Organometallics* **2000**, *19*, 2791.
(11) Schönherr, H.; Beulen, M. W. J.; Bürgler, J.; Huskens, J.; van Veggel, F. C. J. M.; Reinhoudt, D. N.; Vancso, G. J. *J. Am. Chem. Soc.* **2000**, *122*, 4963.
(12) For a recent investigation of the weak binding interactions between oxidized ferrocene and β-cyclodextrin, see: Moozyckine, A. U.; Bookham, J. L.; Deary, M. E.; Davies, D. M. *J. Chem. Soc., Perkin Trans. 2* **2001**, 1858.
(13) Castro, R.; Cuadrado, I.; Alonso, B.; Casado, C. M.; Morán, M.; Kaifer, A. E. *J. Am. Chem. Soc.* **1997**, *119*, 5760.
(14) Cardona, C. M.; McCarley, T. D.; Kaifer, A. E. *J. Org. Chem.* **2000**, *65*, 1857.
(15) Wang, Y.; Mendoza, S.; Kaifer, A. E. *Inorg. Chem.* **1998**, *37*, 317.
(16) Gonzalez, B.; Casado, C. M.; Alonso, B.; Cuadrado, I.; Morán, M.; Wang, Y.; Kaifer, A. E. *Chem. Commun.* **1998**, 2569.
(17) Casado, C. M.; González, B.; Cuadrado, I.; Alonso, B.; Morán, M.; Losada, J. *Angew. Chem., Int. Ed.* **2000**, *39*, 2135.
(18) González, B.; Cuadrado, I.; Casado, C. M.; Alonso, B.; Pastor, C. J. *Organometallics* **2000**, *19*, 5518.

10.1021/om0202064 CCC: $22.00
Publication on Web 07/10/2002

Scheme 1. Synthesis of Compound 2

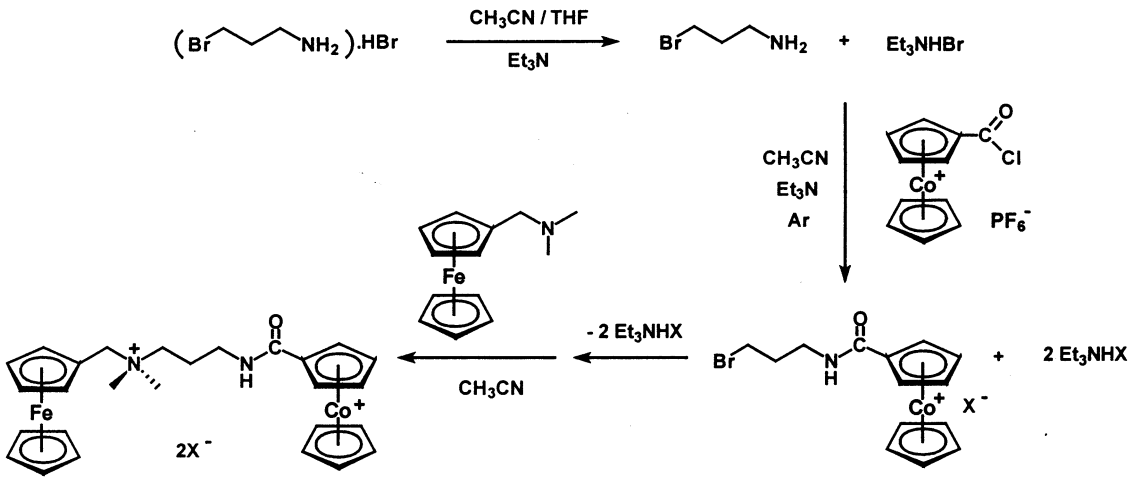

pounds **1** and **2**, their electrochemical properties, and their binding interactions with β-CD hosts in aqueous solution.

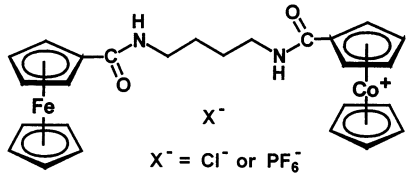

1

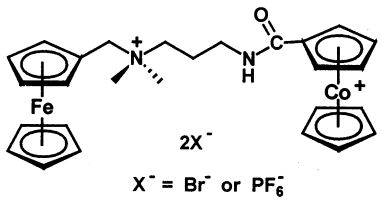

2

Results and Discussion

Synthesis and Characterization. The synthesis of compound **1** has been described in detail in a previous note in which we discussed the best synthetic approach to this heterobimetallic ferrocene−cobaltocenium complex via condensation reactions.[18] Compound **2** was targeted for synthesis due to the positively charged nitrogen in the tether that links the two metallocene units, a structural feature that was anticipated to increase the solubility in aqueous media, especially in the fully reduced cobaltocene form. The preparation of **2** followed the reaction steps shown in Scheme 1. It is worthwhile to point out that special care has to be taken in order to circumvent certain undesirable inter- and intramolecular bimolecular nucleophillic substitution (S_N2) reactions. First, the HBr protecting group in 3-bromopropylamine hydrobromide was removed using an equimolar amount of triethylamine as acceptor base, and without delay, the primary amine was condensed with 1-chlorocarbonylcobaltocenium hexafluorophosphate, in the presence of one additional equivalent of triethylamine to scavenge the HCl generated in this reaction. Immediately after the removal of the triethylammonium byproducts, the terminal bromide intermediate *N*-(3-bromopropyl)cobaltocenium amide was reacted with an excess of *N*,*N*-dimethylaminomethylferrocene. The bromide salt of the quaternized heterobimetallic compound **2** was successfully separated by column chromatography on Sephadex-LH as a very hygroscopic, shiny orange solid. With the aim of obtaining crystals suitable for crystallographic analysis, **2** was also isolated after counterion exchange as its hexafluorophosphate salt, **2·(PF$_6$)$_2$**.

The structure of the novel heterobimetallic complex **2** was straightforwardly determined on the basis of ^{1}H and ^{13}C NMR spectroscopy, electrospray mass spectrometry (ESI-MS), and elemental analysis. The ^{1}H NMR spectrum of **2** (in DMSO-d_6) shows the pattern of resonances characteristic of cyclopentadienyl derivatives in the expected regions for each of the metallocenes, at 5.8−6.3 ppm for the cobaltocenium moiety and at 4.2−4.5 ppm for the ferrocene moiety. These two sets of resonances show a 1:1 ratio of integrated intensities, which is consistent with the simultaneous presence of a ferrocenyl and cobaltocenium unit in **2**. The assignment of the peaks corresponding to the methylene carbons of the connecting bridge in the ^{13}C NMR spectrum has been confirmed by HMQC. The ESI mass spectrum of compound **2·(PF$_6$)$_2$** provided additional confirmation for the structure and showed the peaks corresponding to the successive loss of the two PF_6^- anions, observed at *m*/*z* 661 and 515, as well as other peaks (at lower *m*/*z* ratios) that can be assigned to reasonable fragmentation products. All the fragments that produce a peak in the mass spectrum result from cleavage of the bonds between the quaternary ammonium nitrogen and adjacent methylene carbons.

The structure of the heterobimetallic compound **2** was corroborated via X-ray crystallographic analysis. Single crystals of **2·(PF$_6$)$_2$** suitable for crystallographic analysis were grown by slow diffusion of cyclohexane into a dilute solution of the compound in water. The molecular structure of **2·(PF$_6$)$_2$** is illustrated in Figure 1, and selected crystallographic data are given in Table 1. In the structure of **2·(PF$_6$)$_2$** the bridge adopts a bent conformation and the main axes of the metallocene groups are oriented almost perpendicular to one another. The cyclopentadienyl rings in both metallocenes are planar and nearly parallel and exhibit an almost

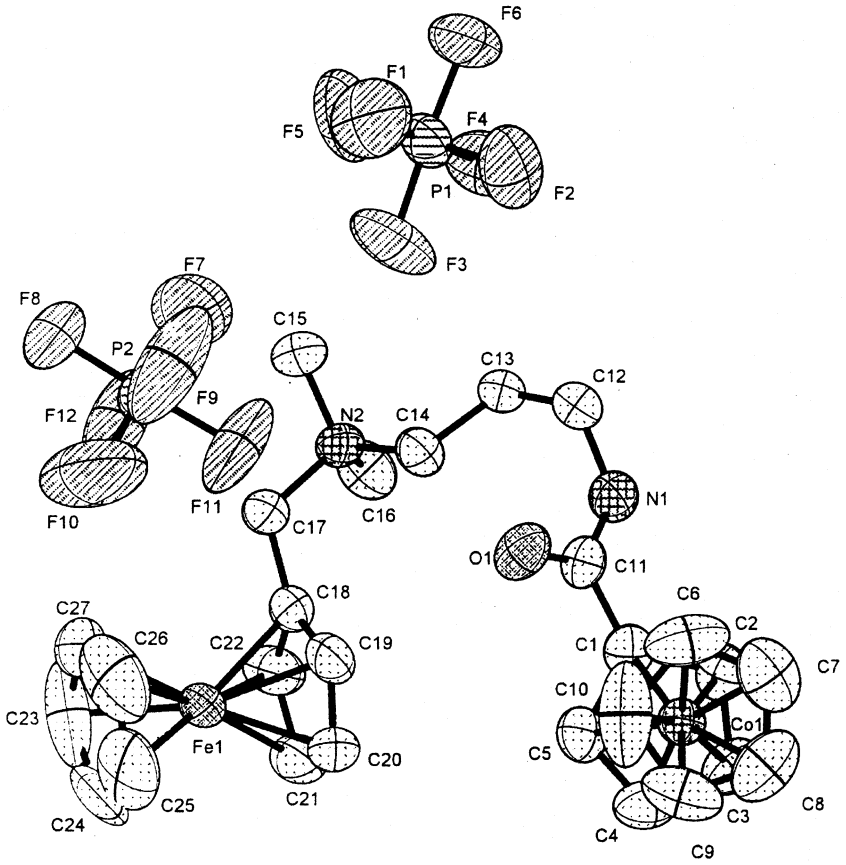

Figure 1. Molecular structure of the heterobimetallic compound **2·(PF$_6$)$_2$** (50% thermal ellipsoids). Selected bond lengths (Å) and bond angles (deg): Co(1)−C(Cp$_{C(1)-C(5)}$) = 2.032(3), Co(1)−C(Cp$_{C(6)-C(10)}$) = 2.007(8), Fe(1)−C(Cp$_{C(18)-C(22)}$) = 2.028(8), Fe(1)−C(Cp$_{C(23)-C(27)}$) = 2.014(6), C(1)−C(11) = 1.490(7), C(17)−C(18) = 1.487(6), C(11)−N(1)−C(12) = 122.7(4), C(17)−N(2)−C(14) = 107.9(3), N(1)−C(11)−C(1) = 115.1(4), N(2)−C(17)−C(18) = 115.6(4). Cp = cyclopentadienyl ring.

Table 1. Crystal Data and Structure Refinement for 2

formula	$C_{27}H_{33}CoFeN_2OP_2F_{12}$
w	806.27
cryst size (mm)	0.20 × 0.13 × 0.07
cryst syst	monoclinic
space group	$P2_1$
a (Å)	6.75700(10)
b (Å)	13.2078(2)
c (Å)	18.1298(3)
β (deg)	97.3010(10)
volume (Å^3), Z	1604.88(4), 2
density (calcd; g/cm^3)	1.668
abs coeff (mm^{-1})	9.500
radiation	graphite-monochromated Cu Kα (λ = 1.54178 Å)
F(000)	816
θ range for data collection, (deg)	2.46 to 70.43
limiting indices	$-8 \le \_h \le 8$, $-15 \le k \le 13$, $0 \le l \le 21$
no. of reflns collected	4851
no. of ind reflns	4851 (R_{int} = 0.0000)
refinement method	full-matrix least-squares on F^2
no. of data/restraints/params	4851/1/419
goodness of fit on F^2	0.925
R_1,[a] wR_2[b] ($I > 2\sigma(I)$)	0.0382, 0.0856
R_1,[a] wR_2[b] (all data)	0.0455, 0.0880
extinction coeff	0.00000(10)
largest diff peak and hole (e$^-$/ Å^3)	0.390 and −0.197

[a] $R_1 = \sum||F_o| - |F_c||/\sum|F_o|$. [b] $wR_2 = \{\sum[w(F_o^2 - F_c^2)^2]/\sum[w(F_o^2)^2]\}^{1/2}$.

eclipsed conformation. The Co−C and Fe−C (cyclopentadienyl ring) average distances are similar to those reported for other cobaltocenium and ferrocene complexes.[18]

Electrochemistry. The voltammetric behavior of compounds **1** and **2** on glassy carbon working electrodes was investigated in 0.1 M NaCl solutions. Figure 2A (solid line) shows the current−potential trace obtained with compound **1**. This cyclic voltammogram has two main features. In the anodic potential range, a reversible wave that corresponds to the one-electron oxidation of the ferrocene residue is clearly observed. The half-wave potential ($E_{1/2}$) for this electrochemical process is 0.42 V vs SSCE. In the negative portion of the voltammogram, a slightly distorted reduction wave is associated with a very sharp anodic spike on scan reversal. These features correspond to the one-electron reduction of the cobaltocenium subunit. As is often the case with cobaltocenium derivatives, reduction leads to an uncharged, neutral species, which precipitates on the electrode surface.[15] The reoxidation of the precipitated material results in the characteristic desorption spike observed on the reverse, anodic-going scan. Table 2 lists some parameters obtained from the voltammetric behavior of **1**. However, its hydrophobic character after one-electron reduction leads to the already described precipitation effects and hinders the quantitative investigation of its electrochemical reduction.

These findings led us to the design and preparation of a more water-soluble ferrocene−cobaltocenium complex, compound **2**, which maintains a positive charge in its structure regardless of the oxidation state of the

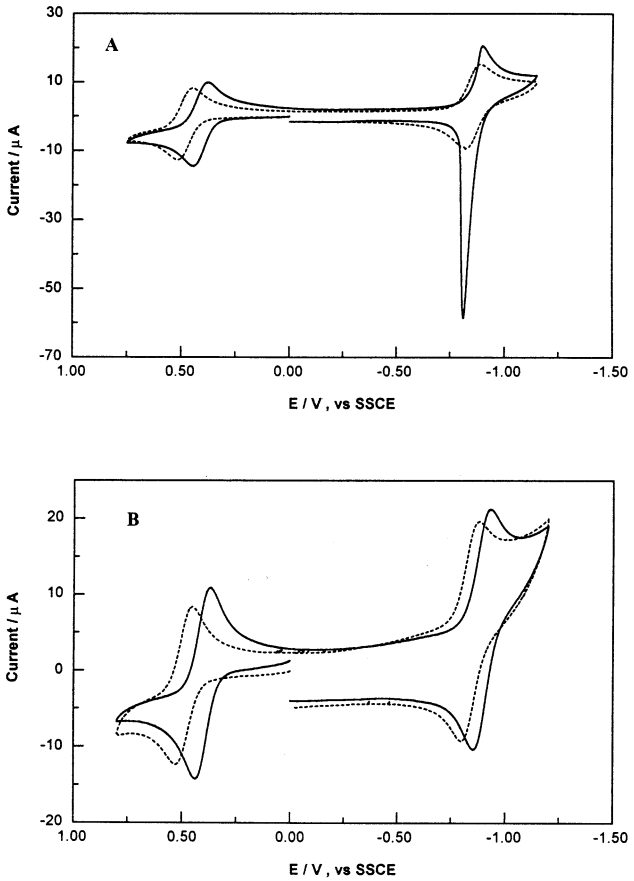

Figure 2. Cyclic voltammograms (at 0.1 V/s) on glassy carbon (0.07 cm^2) of 1.0 mM (A) compound **1** and (B) compound **2**, in 0.1 M NaCl (solid line). The dotted line voltammograms were obtained after the addition of 10.0 mM β-CD.

Table 2. Thermodynamic and Electrochemical Parameters Obtained from Digital Simulations of the Cyclic Voltammetric Responses of Aqueous Solutions Containing Compound 1 or 2 and β-CD at 25 °C, in 0.1 M NaCl

	compound **1**	compound **2**	
parameter	Fc	Fc	Cb
$E_{1/2}$ (V vs SSCE)	+0.42[a]	+0.41[a]	−0.89[b]
$k°$ (cm/s)[c]		0.5	0.5
D (cm^2/s)[d]	3.6×10^{-6}	4.6×10^{-6}	
$D_{complex}$ (cm^2/s)[e]		3×10^{-6}	
$D_{complex}$ (cm^2/s)[f]		1.5×10^{-6}	
K (L/mol)[g]		3700	900
k_f (M^{-1} s^{-1})[h]		4×10^7	4×10^7

[a] Half-wave potential for the one-electron oxidation of the ferrocene moiety in the compound. [b] Half-wave potential for the one-electron reduction of the cobaltocenium moiety in the compound. [c] Standard rate constant for the corresponding heterogeneous electron transfer process. Any value larger than 0.1 cm/s gives similar results. The reversible character of the electron transfer reactions does not allow the accurate determination of this parameter. [d] Diffusion coefficient for the compound obtained from chronocoulometric measurements. [e] Diffusion coefficient for the inclusion complex with one β-CD in the ferrocene or cobaltocene binding sites. [f] Diffusion coefficient for the inclusion complex with two β-CD. [g] Association equilibrium constant as defined in Scheme 2. [h] Bimolecular association rate constant for CD binding. The value given in the table was taken from previous results on simpler compounds (see, for instance, ref 15).

metallocene centers. The cyclic voltammetric behavior of **2** is shown in Figure 2B (solid line). As it was the case with compound **1**, the reversible, one-electron oxidation of the ferrocene residue is clearly visible ($E_{1/2}$ = 0.41 V vs SSCE) on the anodic portion of the current−potential curve. The cathodic side of the voltammogram reveals another reversible, one-electron reduction wave ($E_{1/2}$ = −0.89 V vs SSCE), and in contrast to the behavior of compound **1**, there is no detectable precipitation of the reduced form. Both heterogeneous electron transfer processes are chemically and electrochemically reversible for **2**. These voltammetric data confirm the increased solubility of **2** in all of its oxidation states, as compared to compound **1**.

The electrochemical results also verify that each metallocene heterobimetallic complex may exist in three different oxidation states, which can be designated by the following abbreviations: Fc^+-Cob^+, Fc-Cob^+, and Fc-Cob, where Fc and Fc^+ stand for ferrocene and ferrocenium, respectively, and Cob^+ and Cob represent cobaltocenium and cobaltocene. These three oxidation states are listed in the order in which they would be formed in a negative-going potential scan. The interconversions between these oxidation states are fast in the cyclic voltammetric time scales used in this work, as would be expected from the fast heterogeneous electron transfer reactions usually associated with the Fc^+/Fc and Cob^+/Cob redox couples.[15]

Binding Interactions with β-CD. The presence of excess β-CD (10 equiv) has a marked effect on the voltammetric behavior of compound **1** (see Figure 2A, dotted line). First, the half-wave potential for the ferrocene oxidation wave shifts to a more positive value, and the currents associated with this wave decrease. These CD-induced changes are well-established indicators for the formation of a stable inclusion complex between the ferrocene form of the dimer and the β-CD host.[6,7,10] The stability of this complex is severely diminished after ferrocene oxidation. On the negative potential region the presence of β-CD has a pronounced effect on the shape of the wave for the one-electron reduction of cobaltocenium; in particular, the sharp spike visible on scan reversal disappears with excess β-CD and the electrochemical process becomes reversible. These CD-induced effects are identical to those previously observed by us in the electrochemical reduction of cobaltocenium[15] and cobaltocenium-containing dendrimers[16] and can be easily explained by the formation of a stable inclusion complex between the reduced cobaltocene and the CD host. We thus conclude that the initial oxidation state of **1** (Fc-Cob^+) exhibits a single binding site for β-CD, that is, the ferrocene center. This binding site is removed upon oxidation to its Fc^+-Cob^+ form, which exhibits no significant binding affinity with β-CD. Conversely, one-electron reduction of **1** produces its Fc-Cob form, which contains two well-defined binding sites for β-CD, the ferrocene and the cobaltocene residues. In principle, the Fc-Cob oxidation state of **1** may form a ternary inclusion complex with two β-CD host molecules.

Compound **2** allows us to circumvent the problems that arise from the precipitation of the Fc-Cob form of **1** on the working electrode surface. Specifically, we wished to complete the investigation of the binding interactions of the Fc-Cob oxidation states with β-CD. Figure 2B (dotted line) shows the current−potential trace obtained with compound **2** in the presence of

excess β-CD host. On the anodic side of the voltammogram, the same CD-induced effects observed with compound **1** are clearly apparent. First, the set of waves corresponding to the one-electron oxidation of ferrocene is shifted to more positive potentials and, second, the currents associated with the anodic and cathodic peaks are depressed. As discussed before, these effects reveal the formation of a stable inclusion complex between Fc-Cob$^+$ and β-CD, which is disrupted upon oxidation to the Fc$^+$-Cob$^+$ form. On the cathodic section of the current−potential trace, the set of waves corresponding to the one-electron reduction of the cobaltocenium residue shift to less negative potential values and exhibit smaller current levels in the presence of the CD host. Qualitatively, these CD-induced effects indicate the formation of a stable inclusion complex between β-CD and the cobaltocene center. Overall, these voltammetric data reveal that the three oxidation states of compound **2** have different guest-binding properties toward β-CD. While fully oxidized **2** (Fc$^+$-Cob$^+$) is not a good guest for the CD host, Fc-Cob$^+$ contains one binding site (the ferrocene center) and the fully reduced form (Fc-Cob) shows two binding sites and the possibility to form ternary complexes with two β-CD molecules. Qualitatively, both heterobimetallic complexes **1** and **2** exhibit similar binding properties as guests for β-CD. However, the higher aqueous solubility of **2** in all of its oxidation states permits a more quantitative investigation of its binding interactions with the CD host.

To interpret quantitatively the voltammetric results and obtain thermodynamic parameters for the corresponding binding equilibria, it is necessary to postulate a detailed mechanism for the electrochemical and chemical processes involved. An acceptable mechanism should lead to the generation of digitally simulated voltammograms that approach closely the experimental voltammograms. When a reasonable mechanism is postulated, the optimization of the fit between the simulated and experimental current−potential curves allows the estimation of the thermodynamic parameters for the complexation equilibria between the three oxidation states of the heterobimetallic complex and β-CD. Here, we assume that the mechanism for the electrochemical reactions of compound **2** in the presence of β-CD can be inferred from the mechanisms previously postulated for the oxidation of ferrocene derivatives[6,7,10] and those for the reduction of cobaltocenium derivatives.[15] The main common feature in all these mechanisms is that no electron transfer reactions take place on the inclusion complexes; that is, complex dissociation always precedes the actual electrochemical conversions. According to this, we propose the mechanism shown in Scheme 2 for the redox conversions of compound **2** in the presence of β-CD.

A cursory examination of the mechanism reveals that the number of possible complexation steps that must be taken into account is rather large. In particular, the host−guest interactions between the fully reduced form of the heterobimetallic complex (Fc-Cob) and β-CD are complicated by the presence of two nonequivalent binding sites. To facilitate the study of the system, we first focused on the host−guest interactions between Fc-Cob$^+$ and β-CD. In terms of Scheme 2, this means that we concentrate our attention on the steps enclosed inside the marked rectangle. Experimentally, we can focus on these processes by narrowing the surveyed potential range to values that are more positive than the half-wave potential for the Fc-Cob$^+$/Fc-Cob redox couple. Under these conditions, there is only one redox couple (ferrocenium/ferrocene) and one chemical equilibrium (binding between Fc-Cob$^+$ and β-CD) to consider, and the voltammetric behavior can be described by a so-called *CE* mechanism, that is, a chemical step (complex dissociation) preceding the electron transfer reaction (reversible one-electron oxidation of the ferrocene center).

Scheme 2. Electrochemical and Chemical Equilibria Involved in the Voltammetric Behavior of the Heterobimetallic Complex 2 in the Presence of β-CD Host

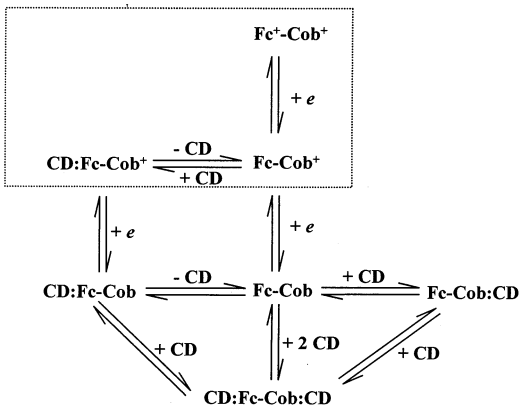

Using this simple mechanism we fitted the experimental voltammograms (anodic potential range) obtained with a fixed concentration of **2** and varying concentrations of β-CD to digitally simulated voltammograms. To generate digital simulations, several parameters must be used to describe the electron transfer and binding equilibria. The parameter values that produced the best simulations are given in Table 2, and comparisons between the simulated and the experimental voltammograms are shown in Figure 3 for two different cases: no CD (Figure 3A) and 10-fold excess of CD (Figure 3B). The agreement between the digitally simulated and the experimental current−potential curves is very good. Notice that the simulated voltammograms reproduce very well the position of the characteristic potentials (peak and half-wave) of the voltammograms. The parameters reported in Table 2 for the complexation equilibrium between Fc-Cob$^+$ and β-CD are in excellent agrement with other values previously reported for binding between ferrocene derivatives and this host.[6,7,8,10]

Scheme 2 shows the complexity of the binding interactions between β-CD and the fully reduced form of **2** (Fc-Cob). It is well known that the error margin of the parameters obtained through simulations of electrochemical data increases quickly with the number of parameters. Instead of attempting to obtain thermodynamic and kinetic parameters for all the chemical steps shown in Scheme 2, we decided to simplify the system using an approximation. We assumed that the binding interactions between Fc-Cob and β-CD can be treated by a simple *EC* mechanism in which the reduction of Fc-Cob$^+$ is followed by the formation of an inclusion complex (Fc-Cob:CD). However, to take into account the presence of the ferrocene binding site, we adjusted the

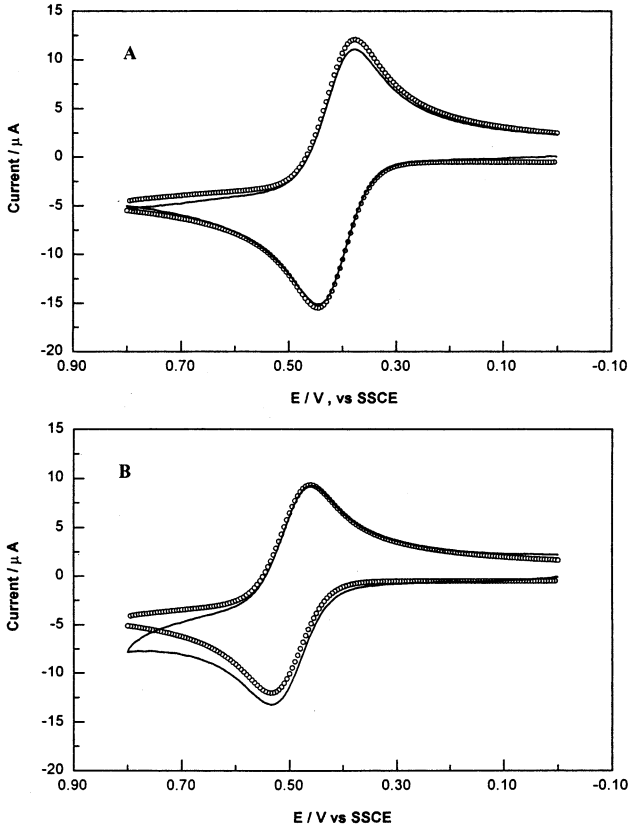

Figure 3. Cyclic voltammograms (at 0.1 V/s) on glassy carbon (0.07 cm^2) of 1.0 mM compound **2** (showing only the Fc/Fc^+ proccess) in 0.1 M NaCl also containing (A) 0.0 mM β-CD and (B) 10.0 mM β-CD. Solid line: experimental voltammogram after background subtraction. Dotted line: digital simulation obtained with the parameter values given in Table 2.

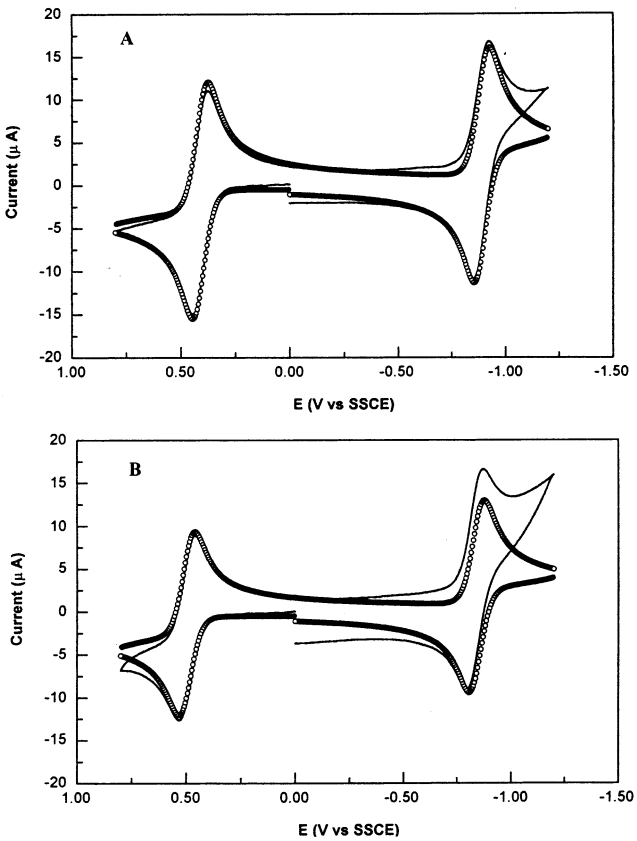

Figure 4. Cyclic voltammogram (at 0.1 V/s) on glassy carbon (0.07 cm^2) of 1.0 mM compound **2** in 0.1 M NaCl also containing (A) 0.0 mM β-CD and (B) 10.0 mM β-CD. Solid line: experimental voltammogram after background subtraction. Dotted line: digital simulation obtained with the parameter values given in Table 2.

total concentration of β-CD to reflect that a fraction of the host would not be available to bind the cobaltocene site, as it would be complexed to the ferrocene site. For this adjustement, we used the previously determined binding constant for the formation of the CD:Fc-Cob^+ inclusion complex. Figure 4 shows examples of the type of fits between simulated (using the parameters given in Table 2) and experimental current−potential curves that we obtained through this approach. The current values measured at the two extremes of the surveyed potential range ($E > 0.6$ V and $E < -0.9$ V) are affected by background processes, such as proton reduction on the cathodic end of the voltammogram, and cannot be fitted closely by our simulations. However, the characteristic potentials observed in the experimental voltammogram are reproduced very satisfactorily by the simulations. In fact, Figure 5 shows that the agreement between the simulated and experimental half-wave potential values is very good and extends over the entire CD concentration range surveyed in our experiments. This verifies that the proposed mechanism and the parameters in Table 2 represent the behavior of the system in a very reasonable fashion. In addition to this, the approach used to analyze the experimental voltammetric data yields thermodynamic parameters for the binding interactions between the three oxidation states of **2** and β-CD that are in good agreement with values previously reported for simpler monomeric guests.[6−8,10,15] Our digital simulations indicate that the

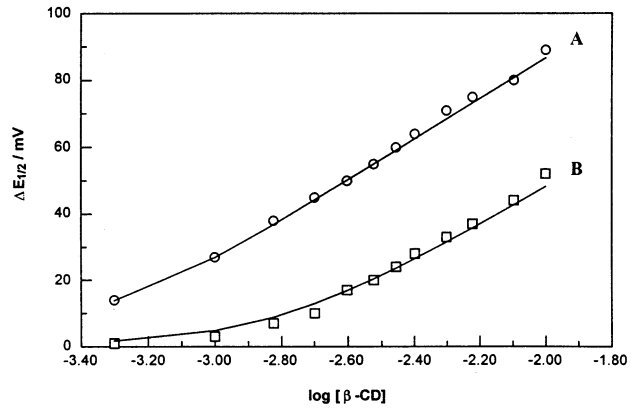

Figure 5. Plots of the CD-induced half-wave potential shifts ($\Delta E_{1/2}$) as a function of the total concentration of β-CD, (A) for the oxidation of the ferrocene in compound **2** (○ experimental data; − simulated values) and (B) for the reduction of the cobaltocenium in compound **2** (□ experimental data; − simulated values).

error margin in the reported binding constant is in the range 10−15%. Due to the complexity of the binding mechanism considered here, we did not attempt to obtain kinetic rate constants for the β-CD association and dissociation processes. Throughout the digital simulations performed in this work, we simply utilized kinetic rate constant values that were taken from prior work on the complexation of simple ferrocene[6] or cobaltocene[15] guests.

Conclusions

Heterobimetallic complexes **1** and **2** have three oxidation states with very different guest properties for binding by β-CD. Qualitatively, both compounds behave similarly, but the increased solubility of **2** allowed us to investigate its complexation to the CD host in a more quantitative fashion. Our findings reveal that the β-CD/**2** host−guest system has three different states accessible by redox conversions affecting compound **2**. The fully oxidized state of **2** (Fc^+-Cob^+) does not interact appreciably with β-CD. The intermediate and most stable oxidation state (Fc-Cob^+) forms a stable 1:1 inclusion complex, in which the host binds the ferrocene site. Finally, the fully reduced state (Fc-Cob) has two binding states and may form 1:1 and 2:1 inclusion complexes with β-CD. Thus, this system constitutes a novel example of *a three-state, host−guest system under redox control*.

Experimental Section

Materials and Equipment. All reactions were performed under an inert atmosphere (prepurified Ar) using standard Schlenk techniques. Solvents were dried by standard procedures over the appropiate drying agents and distilled immediately prior to use. Triethylamine (Merck) was distilled over KOH under Ar. Compound **1** was prepared as previously reported.[18] 3-Bromopropylamine hydrobromide was purchased from Aldrich and *N*,*N*-dimethylaminomethylferrocene from Strem Chemicals. Both compounds were used without further purification. The hexafluorophosphate salt of 1-chlorocarbonylcobaltocenium was prepared as reported by Sheats and Rausch.[19] Chromatographic separation was performed with the use of Sephadex LH-20 (Fluka). NMR spectra were recorded on a Bruker-AMX spectrometer. Chemical shifts are reported in parts per million (δ) with reference to residual solvent resonances. ESI mass spectral analyses were conducted on a 1100 HP-LCMS spectrometer. Elemental analyses were performed by the Microanalytical Laboratory, Universidad Autónoma de Madrid, Madrid, Spain. β-CD was purchased from Cerestar and used as received. The hydrated molecular weight of β-CD (1297.1 g/mol) was used throughout this work. All other chemicals were of the best quality commercially available. Deionized water was further purified by passage through a pressurized, four-cartridge Barnstead Nanopure system to a final resistivity of 18 MΩ cm or higher.

Electrochemical Measurements. All the electrochemical experiments were performed with a BAS 100 B/W workstation (Bioanalytical Systems, West Lafayette, IN). A glassy carbon disk working electrode (0.07 cm^2), tungsten counter electrode, and sodium chloride saturated calomel (SSCE) reference electrode were fitted to a 5 mL, single-compartment electrochemical cell. Digital simulations of the experimental cyclic voltammograms were carried out with the DigiSim 3.03 software package.[20] The surface of the working electrode was polished with a 0.05 μm alumina/water slurry on a felt surface and rinsed with purified water before each cyclic voltammetric run. The solutions for the electrochemical experiments were purged with nitrogen and kept under an inert atmosphere throughout the measurements. Typically, a 1.0 mM solution of the electroactive compound in 0.1 M supporting electrolyte solution (NaCl) was prepared for the electrochemical experiments. The concentration of β-CD in the solution was adjusted to the desired level (within the 0.0−10.0 mM range) by adding carefully weighted amounts of solid β-CD host.

X-ray Crystal Structure Determination. A suitable orange crystal of **2·$(PF_6)_2$** of prismatic shape and dimensions 0.20 × 0.13 × 0.07 mm was located and mounted on a glass fiber with silicone cement in air and placed on a Bruker SMART6000 CCD-based X-ray diffractometer with a monochromatic radiation source (λ = 1.54178 Å). Data were collected at 296 K using continuous $\omega-2B$ scans. A total of 4851 independent reflections (R_{int} = 0.0000) were collected in the range 4.92° < 2θ < 140.86°. The stability of the crystal was tested every 50 with three check reflections that showed only random fluctuations in intensity during data collection. The intensities were corrected for Lorentz and polarization effects. Scattering factors and corrections for anomalous dispersion were taken from a standard source.[21] Calculations were performed using Bruker SHELXTL for NT, version 6.10, a system of programs refining on F^2. The structure was solved by direct methods, and there were no unusual features in this refinement. The hydrogen atom positions were calculated with fixed isotropic contributions at their calculated positions determined by molecular geometry. An absorption correction using an empirical model (SADABS V2.03) was applied. All non-hydrogen atoms were refined with anisotropic thermal parameters.

Synthesis of 2. A recently prepared solution of 3-bromopropylamine hydrobromide (0.55 g, 2.5 mmol) and Et_3N (0.25 g, 2.5 mmol) in CH_3CN/THF (1:1) (60 mL) and another solution of Et_3N (0.25 g, 2.5 mmol) in CH_3CN (50 mL) were added dropwise to a solution of 1-chlorocarbonylcobaltocenium hexafluorophosphate (1.00 g, 2.5 mmol) in CH_3CN (40 mL) maintained under an argon atmosphere. The reaction mixture was stirred for 2 h under argon at room temperature. After removal of the solvent, the resulting residue was redissolved in CH_3CN and cooled to −30 °C in order to precipitate the triethylammonium salt byproduct. Once the triethylammonium salt had been removed, the product was dissolved in CH_3CN (40 mL), and to this solution was added dropwise *N*,*N*-dimethylaminomethylferrocene (1.23 g, 5.1 mmoL) in CH_3CN (15 mL). The stirring was continued overnight. The solvent was removed under vacuum, and the resulting residue was purified by column chromatography on Sephadex LH-20. Using CH_3CN as eluent, the excess of *N*,*N*-dimethylaminomethylferrocene and the salt of *N*,*N*-dimethylammoniummethylferrocene were separated in the first and second fractions, respectively. An orange band containing the desired compound was separated using CH_3CN/EtOH (40:2) as eluent, and after drying under vacuum the bromide salt of compound **2** was obtained as a very hygroscopic, shiny orange solid in 29% yield. To obtain the corresponding hexafluorophosphate salt, a portion of this solid was redissolved in a small quantity of water and a solution of NH_4PF_6 was added dropwise. The hexafluorophosphate salt of **2** was obtained as a crystalline orange solid. ^{1}H NMR (500 MHz, DMSO-d_6, 50 °C): δ (ppm) 9.44 (t, 1H, CON*H*,), 6.48 (pseudotriplet, 2H, $C_5H_{4[Cob]}$), 5.96 (pseudotriplet, 2H, $C_5H_{4[Cob]}$), 5.90 (s, 5H, $C_5H_{5[Cob]}$), 4.56 (pseudotriplet, 2H, $C_5H_{4[Fcl]}$), 4.47 (s, 2H, FcCH_2N), 4.37 (pseudotriplet, 2H, $C_5H_{4[Fcl]}$), 4.27 (s, 5H, $C_5H_{5[Fcl]}$), 3.34 (pseudoquartet, 2H, CONHCH_2), 3.28 (m, 2H, CH_2CH_2N), 2.93 (s, 6H, N(CH_3)$_2$), 2.51 (m, 2H, $CH_2CH_2CH_2$). ^{13}C{^{1}H} NMR (125.76 MHz, DMSO-d_6, 25 °C): δ (ppm) 162.5 (*C*ONH), 94.4 ($C_5H_{4[Cob]}$), 86.9 ($C_5H_{5[Cob]}$), 86.6 ($C_5H_{4[Cob]}$), 85.1 ($C_5H_{4[Cob]}$), 73.8 ($C_5H_{4[Fcl]}$), 72.9 ($C_5H_{4[Fcl]}$), 70.9 ($C_5H_{4[Fcl]}$), 69.9 ($C_5H_{5[Fcl]}$), 64.7 (FcCH_2N), 61.3 (NCH_2CH_2), 50.1 (N(CH_3)$_2$), 37.3 (CH_2NHCO), 23.1 (CH_2CH_2-CH_2). ESI-MS for **2·$(PF_6)_2$**: *m*/*z* 661.1 [M − PF_6^-]$^+$, 515.2 [M − 2PF_6^- − H$^+$]$^+$, 317.1 [M − 2PF_6^- − FcCH_2^+]$^+$, 272.1 [M − 2PF_6^- − FcCH_2N(CH_3)$_2$ − H$^+$]$^+$, 199.1 [FcCH_2]$^+$. Anal. Calcd for $C_{27}H_{33}ON_2FeCoP_2F_{12}$: C, 40.19; H, 4.09; N, 3.47. Found: C, 40.15; H, 4.08; N, 3.59.

(19) Sheats, J. E.; Rausch, M. D. *J. Org. Chem.* **1970**, *35*, 3245.
(20) Rudolph, M.; Reddy, D. P.; Feldberg, S. W. *Anal. Chem.* **1994**, *66*, 589A.
(21) *International Tables for X-ray Crystallography*; Kynoch Press: Birmingham, England, 1974; Vol. 4.

Acknowledgment. The authors wish to thank the National Science Foundation (to A.E.K., CHE-9982014), the Spanish Dirección General de Investigación (PB97-0001 and BQU2001-0210), and the Comunidad de Madrid (07M/0066/2000) for the generous support of this work. B.G. acknowledges the Consejería de Educación y Cultura de la Comunidad de Madrid for a doctoral fellowship. A.E.K. is grateful to the IBERDROLA Program for Visitor Professors. We are grateful to C. J. Pastor (Universidad Autónoma de Madrid) for valuable discussions on X-ray crystal structure determination.

Supporting Information Available: Tables of all bond distances and angles, displacement parameters, atomic coordinates, and torsion angles for **2**. This material is available free of charge via the Internet at http://pubs.acs.org.

OM0202064